JTTEE5 4:34-40

Modeling the Deposition Process of Thermal Barrier Coatings

J.H. Harding, P.A. Mulheran, S. Cirolini, M. Marchese, and G. Jacucci

Thermal barrier coatings produced by plasma spraying have a characteristic microstructure of lamellae, pores, and cracks. The lamellae form when particles splash onto the substrate. As the coating grows, the lamellae pile on top of one another, producing an interlocking structure. In most cases the growth is rapid and chaotic, resulting in a microstructure characterized by pores and cracks. This paper presents an improved model for the deposition process of thermal barrier coatings. The task of modeling the coating growth is divided into two parts. First, a description of the particle on arrival at the film is given based on the available theoretical, numerical, and experimental findings. Second, a set of physically based rules for combining these events to obtain the film is defined and discussed. The splats run along the surface and are permitted to curl up (producing pores) or to interlock. The computer model uses a mesh to combine these processes and build the coating. The proposed model can be used to predict microstructures and hence to correlate the properties of these coatings with the parameters of the process used to make them.

1. Introduction

COATING behavior frequently depends on microstructural details that result from the coating production method. Thermal barrier coatings produced by plasma spraying have a characteristic microstructure of lamellae, pores, and cracks. The lamellae form when particles splash onto the substrate. The time required for a particle to splash is sufficiently short (about 10 μ s (Ref 1-3) that each splash can be considered to be independent of the others. As the coating grows, the lamellae pile on top of one another, producing an interlocking structure. In most cases the growth is rapid and (in a loose sense) chaotic. Furthermore, residual stresses are built into the system (mainly through thermal expansion mismatch). The result is pores and cracks.

The problem of simulating plasma spraying can thus be divided into three parts: the study of the plasma and particles in flight, the splashing event, and the piling up of splats to form the coating. Much work has already been done on the first part of the problem (see, for example, Ref 1, 4, and 5). This paper will discuss the other two.

A number of previous attempts have been made to model the porosity creation mechanism. Knotek and Elsing (Ref 6) constructed a coating model that assumed that pores were created between the splats, but they did not generate their pores by any physical mechanism.

Other workers (Ref 7) have suggested that the trapping of plasma gas may be important. In this model, the splashing particle traps the gas between the base of the particle and the rough substrate. The gas is compressed by the particle motion. The shape of the pore depends on whether or not the splat wets the substrate. There are two difficulties. First, without a complete calculation of the splashing process, the percentage of the kinetic energy of the incoming particle available to compress the gas remains unknown. However, the kinetic energy available must be small, or all pores would be destroyed. Indeed, Madejski (Ref 8), in his analytical calculation of the splat diameter/particle diameter ratio, assumed that the percentage was zero; all the kinetic energy was dissipated to the surrounding structure. Without a value for this percentage, Fukanuma's estimate (Ref 7) of the importance of trapped gas must remain arbitrary. Also, the discussion of wetting can only be of importance at the coating/substrate boundary since all liquids wet their own solid phase, if no surface films exist.

Pekshev and Murzin (Ref 9) have classified the different types of porosity. They present a set of analytical calculations for three of the pore classes they define: interlamellar pores, intergranular pores, and microcracks. They claim that these three types of pores form the bulk of the porosity.

A large number of studies of coating microstructure have been undertaken (e.g., Ref 10-12). These studies have identified the influence of such factors as interlamellar adhesion and microcracking on coating properties. Kuroda et al. (Ref 13) have demonstrated the importance of the stress generated when the splashed particle cools on the substrate (quenching stress) in the creation of pores and cracks. Their experiments also show the importance of microstructure in terms of mechanical properties. However, very few studies have produced detailed statistical correlations between microstructural features and coating properties. There are too many features and few methods of unambiguously identifying them. Porosity is one feature that can be measured.

We have already presented (Ref 14) a model to calculate the porosity of thermal barrier coatings as a function of process parameters. In this paper we extend and improve the model.

The task of modeling the coating growth is divided into two parts. First, a description of the particle on arrival at the film is given, based on the available theoretical, numerical, and experimental findings. Each particle splashes to produce a thin splat. This splat runs along the surface and is permitted to curl up during cooling. Porosity is produced if the gap between the curled-up splat and the surface is not filled by subsequent splats. A

Keywords: finite-element method, fluid flow and heat transfer, modeling, particle impact and splat geometry, porosity generation model, thermal barrier coatings

J.H. Harding and **P.A. Mulheran,** Theoretical Studies Department, AEA Technology, Didcot, Oxon OX11 0RA, U.K.; **S. Cirolini, M. Marchese,** and **G. Jacucci,** University of Trento, Laboratory of Computer Science Engineering, I-38068 Rovereto (TN), Italy.

detailed investigation of the cooling process for each lamella is presented in Section 2. Second, a set of physically based rules for combining the splashing events to obtain the film is defined and discussed in Section 3. The computer model uses a mesh to build the coating structure. The proposed model can be used to predict microstructures and hence to correlate the properties of these coatings with the parameters of the process used to make them.

2. Cooling of a Single Particle

As described earlier, when a molten particle impacts the substrate surface, it splashes to form a thin lamina and solidifies in a very short time. This process determines both the microstructural (crystalline phases, crystallite size) and the macroscopic characteristics (porosity, adhesion) of the coating. These features may be subsequently modified by thermal treatments such as aging or sintering.

2.1 *Impact Process*

The impact process for plasma spray conditions has been investigated recently both experimentally (Ref 15, 16) and by numerical simulation (Ref 2, 3, 16). Our description of the impact is based on the Madejski model and on improvements derived from this new experimental and numerical evidence (Ref 3, 15, 16).

Madejski (Ref 8) showed that, given his assumptions, the ratio ξ of the splat diameter to the original particle diameter, also called "flattening degree," is given by:

$$\xi = A\left(\frac{\rho V d}{\eta}\right)^{0.2} \qquad \text{(Eq 1)}$$

where ρ is the density, η is viscosity, d is particle density, V is velocity, and A is a dimensionless constant (equal to 1.2941 in Madejski's model). Thus, splat diameter increases as the diameter and velocity of the original particle increases. Recent experimental and numerical calculations (Ref 3, 15, 16) indicate that Madejski overestimated A; satisfactory agreement with experiments and simulations are obtained with a value for A = 0.925 in Eq 1 (Ref 3). In this paper, the impact process is described based on the use of Eq 1 and our proposed value for A.

After impact and solidification the lamina cools. The peripheral part of the lamina detaches from the substrate surface, while the central part of the lamina breaks across its thickness instead of detaching from the surface (Ref 17). This behavior is confirmed by crystallographic characterization of single laminae (Ref 12, 18), which showed the lamina boundaries to be in poor contact with the underlying surface.

Stress development across the lamina is followed using a simple elastic model. The central part of the lower surface of the cylinder, a circular area of diameter D_1, is presumed to adhere strongly to the underlying surface. The other part of the lower surface of the cylinder, beyond the contact area, is assumed to have no adhesion with the substrate surface. Lamina microcracking is not taken into account explicitly. Instead, a sensitivity study on the influence of the contact parameter ($f = D_1/D$) on the curling process has been performed. Therefore, the parameters that fully describe the lamina model are the diameter D, the thickness h, and the contact parameter f. Standard finite-element methods are used to perform the calculations.

2.2 *Simulation of Thermal Changes*

A thermal calculation is first performed to obtain the temperature distribution for the subsequent mechanical calculation. The initial temperature is assumed to be the material solidification temperature (T_{melt} = 2900 K), and, as a first approximation, it is assumed to be uniform across the lamina thickness. The following boundary conditions were imposed for the thermal calculations:

- On the lower surface of the lamina, thermal conduction was assumed to take place between the part of the lamina in contact with the substrate and the substrate. The substrate has been modeled both as a thermal sink (i.e., body at a constant temperature, T_{surf}) and as a separate body in thermal contact with the lamina. The range of values of T_{surf} that have been investigated lie between 400 and 800 K, values typical for plasma-sprayed coatings (Ref 19). The thermal contact resistance at the interface was taken to be 10^{-4} W^{-1}/m^2 · K.
- On the remaining surface of the lamina, heat exchange was assumed to take place by both convection and radiation toward the surrounding gas. Gas temperature was held constant (two values have been investigated: 1500 and 2000 K). A convection coefficient of 10^3 W · m^{-2}/K^{-1} was used. The lamina emissivity was assumed to be 0.5.

The information gained from the thermal simulation was used to structurally model the stresses in the lamina during cooling. In this simple elastic model the two calculations can be decoupled. However, the same model can be also used in the future for coupled simulations if nonlinear terms (material properties, boundary conditions, etc.) are implemented. At present the lamina is assumed to be fully elastic, with the material properties typical for dense zirconia: E = 200 GPa, ν = 0.23. Boundary conditions for the mechanical model were taken as follows: The area of the lamina in contact with the substrate is fixed to the underlying surface (assumption of strong adhesion), and the remaining part is free to move up. A unilateral condition was used to prevent the lamina from penetrating the substrate, which was modeled as a rigid surface.

As expected, most of the heat content of the cooling particle is dispersed into the substrate through the contact in the central zone of the lamina. The cooling rate is insensitive to changes in the surrounding gas temperature. Under the conditions studied, convection and radiation are far less effective than the interfacial conduction in extracting heat from the lamina. The time of cooling is therefore controlled by the contact parameter f, the substrate surface temperature T_{surf}, and the thermal contact resistance at the interface. Moreover, lamina cooling is not uniform. First, the central part of the lamina, which has good adhesion with the surface, is rapidly cooled, requiring less than 100 μs to reach a temperature very close to the substrate temperature. This time does not depend on the amount of contact and is also the cooling time for a full adhering lamina. Figure 1 shows a typical evolution of the temperature profile in the lamina during cooling. In a second phase, the outer part of the lamina cools by the conduction of heat toward the central part. This step is influenced both by the contact parameter and by the lam-

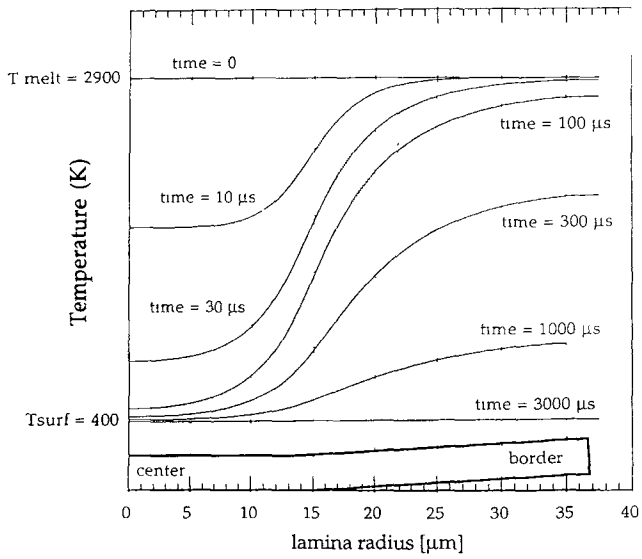

Fig. 1 Evolution of temperature radial profile during cooling

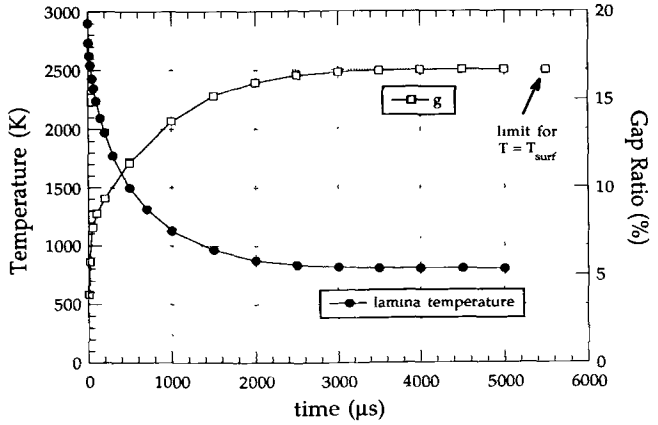

Fig. 2 Typical evolution of gap ratio (g) and lamina temperature

ina thickness. The lamina boundary requires about 1000 μs to reach the temperature of the center.

The total cooling time is always shorter than the mean time between two overlapping impacts, roughly estimated as $h/(2R)$, where R is the growth rate of the thickness of the coating deposited (μm/s). The peak deposition rate can be assumed to be on the order of 10^3 μm/s, and the lamina thickness is a few microns, so the mean time between overlapping splats should be on the order of 10^4 μs. The cooling time for the lamina is thus at least an order of magnitude lower than the mean time between the arrival of two particles in the same place.

2.3 *Development of Curling and the Gap Ratio*

The simulations show that as the lamina cools, its periphery curls away from the substrate. The upper side of the lamina tends to shrink more than the side in contact with the substrate, which is prevented from shrinking by adhesion. A stress gradient develops between the upper part, which is free from stress, and the lower, which is in tension, causing the lamina to curl. As a result, a gap develops between the lamina and the substrate. We can define a gap ratio, g, associated with this process as the ratio of the volume under the lamina opened up by the curling to the total volume of the lamina. Combined with the rules of the deposition model described in Section 3, the gap ratio is related to the final porosity of the coating.

Figure 2 shows the development of g as the temperature decreases. The limiting value for $T = T_{surf}$ was calculated using a static calculation and corresponds to the gap ratio resulting from a lamina completely cooled to the temperature of the substrate. The splats formed under typical plasma spraying conditions are thin and small. Thermal calculations show that they reach equilibrium with the substrate before being disturbed by other impact events.

If the behavior is assumed to be simply elastic, deformation by thermal loads does not depend on the rate of temperature change. In this case, it is unnecessary to follow the whole thermal history of the lamina, and the final value for the gap ratio can be determined by a single-step static calculation. In this case g does not depend on the lamina size, but only on the aspect ratio D/h. Under these assumptions and simplifications, the parameters determining the final gap ratio reduce to three:

- The contact parameter, f
- The lamina aspect ratio, D/h
- The temperature drop between the impacting particle and the surface, ΔT

A complete investigation in the parameter space for the three parameters has been performed. Results are fed into the subsequent deposition model (Section 3). Typical data are shown in Fig. 3 and 4.

In all cases the gap ratio increases as the substrate temperature is held cool, thus leading to higher possible porosity in the coatings (verified experimentally in Ref 20).

The curling of the deposited lamina is thus a suitable mechanism for the formation of porosity in a coating deposited by plasma spraying. Porosity created by the present mechanism is expected to be greater when the substrate surface is held at cooler temperatures and when the splats obtained from the particle impact are thin and have little contact with the substrate.

3. Deposition Model

The deposition model has been discussed previously (Ref 14). We shall repeat the main points here and discuss improvements to the model. The model consists of three parts: the substrate and coating already deposited on it, the characteristics of the arriving particles, and the implementation of the splashing model described earlier to build up the coating.

Two features of the substrate are important: roughness and surface temperature. Thus, two kinds of calculation are necessary. The surface roughness is described by a fractal—defined by the maximum roughness and the number of times the surface crosses a mean line. The surface temperature of the substrate (and subsequently the coating) are calculated by a simple finite-difference calculation using a method similar to that of Pawlowski et al. (Ref 19). Two cases are considered. The first ignores the possibility of cooling the coating during spraying; the second assumes that the coating is cooled by an air jet.

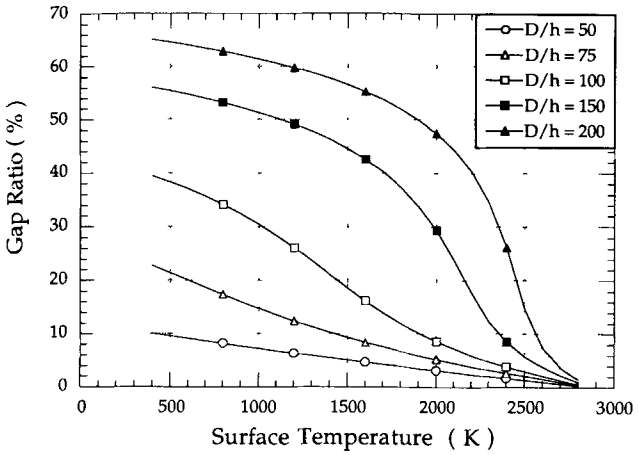

Fig. 3 Gap ratio (g) as a function of surface temperature and lamina aspect ratio (D/h)

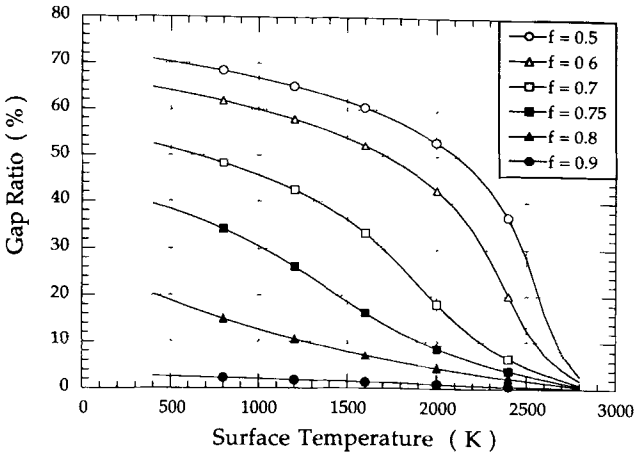

Fig. 4 Gap ratio (g) as a function of surface temperature and contact parameter (f)

The deposition model assumes that the splat follows the shape of the underlying layer for the central region of the splat (the contact area discussed earlier). Beyond this region the splat can curl up, provided that it is not interlocked with another splat above it. The amount of curling is determined by the calculations discussed in the previous section.

The calculation operates as follows. First, the splat is laid along the surface (case A, see Table 1 and Fig. 5). Its length is given by Eq 1. The splat follows the surface closely but not exactly; roughness and pores on the order of the splat thickness are ignored (case B). If the splat can fill gaps in the surface layer without flow reversal, it does so (cases C to E). This is known as interlocking. Our previous calculations (Ref 14) produced spurious vertical correlations between pores. These have been removed by ensuring that the splats remain continuous throughout the calculation. Once the splat has been laid down, the part beyond the contact area (and unaffected by any pinning induced by interlocking) is permitted to curl up using the calculations discussed in the previous section (cases F and G).

Partially melted particles are dealt with by dividing the problem in two. The melted part spreads as discussed earlier. The unmelted part forms a hemisphere on the surface. Completely unmelted particles also form hemispheres, but may bounce off if they hit a previously unmelted region (cases H to L).

Information about the characteristics of incoming particles is required—in particular, the velocity and temperature of the particles as a function of their radius and other process parameters, such as the distance of the gun from the substrate and the power of the plasma torch. Most of this can now be calculated as shown by the studies cited above. For the present, correlations obtained experimentally (Ref 1) are used.

4. Results

Modeled microstructures are shown in Fig. 6. The calculations use a variety of mesh sizes. For convenience, these are reduced to a 512 by 512 pixel grid for plotting purposes.

Figure 6(a) shows the typical features of a plasma-sprayed coating. The long cracklike pores between the laminae are caused by failure of the laminae to stick to one another. Larger, more spherical pores also form when laminae do not stack together properly. This may happen spontaneously or be caused by the presence of unmelted material. Figure 6(b) shows the effect of changing the assumption about the contact area between the splat and the underlying surface. Figure 6(a) assumes that this takes values randomly between 0.2 and 0.8 of the total area of the splat, whereas Fig. 6(b) assumes that this value is fixed at 0.2. This enables a far more regular packing of the splats and eliminates the large spherical pores.

It is interesting to compare the results with previous work (Ref 14). In addition to the differences to the rules noted above, the previous study used the simple Madejski correlation (see Eq 1) with an "A" constant of 1.2941; the present study uses the smaller constant of 0.925, obtained by fitting to the numerical calculations discussed in Section 2. This has the effect of reducing the diameter of the splats produced and hence reducing the

Table 1 Summary of rules of deposition model

Case	Rule
A	Splat is laid along the surface following Eq 1
B	Pores one splat thickness below are destroyed (hammering of porosity); splat is constructed from the impact point outward and follows the surface.
C	If splat encounters a dead end, it fills the space available and then flows over the outer surface above (interlocking mechanism).
D	Splat can cover roughness created by other splats.
E	If splat comes to a vertical drop, it falls straight down until finding the surface again.
F	Splat is then permitted to curl up, provided that it is in the topmost layer.
G	If the underlying region contains a large peak, this can pin the splat; curling is calculated with respect to the peak.
H	Unmelted particles form hemispheres on the coating.
I	Hemisphere is assumed to lie on the mean line of the surface; cavities below will be filled.
J, K	Unmelted particles are assumed not to adhere to the substrate surface or to one another; if they hit either of these, they bounce off.
L	A partially melted particle is divided into two parts: the melted part follows rules A to G; the unmelted part, rules I to K.

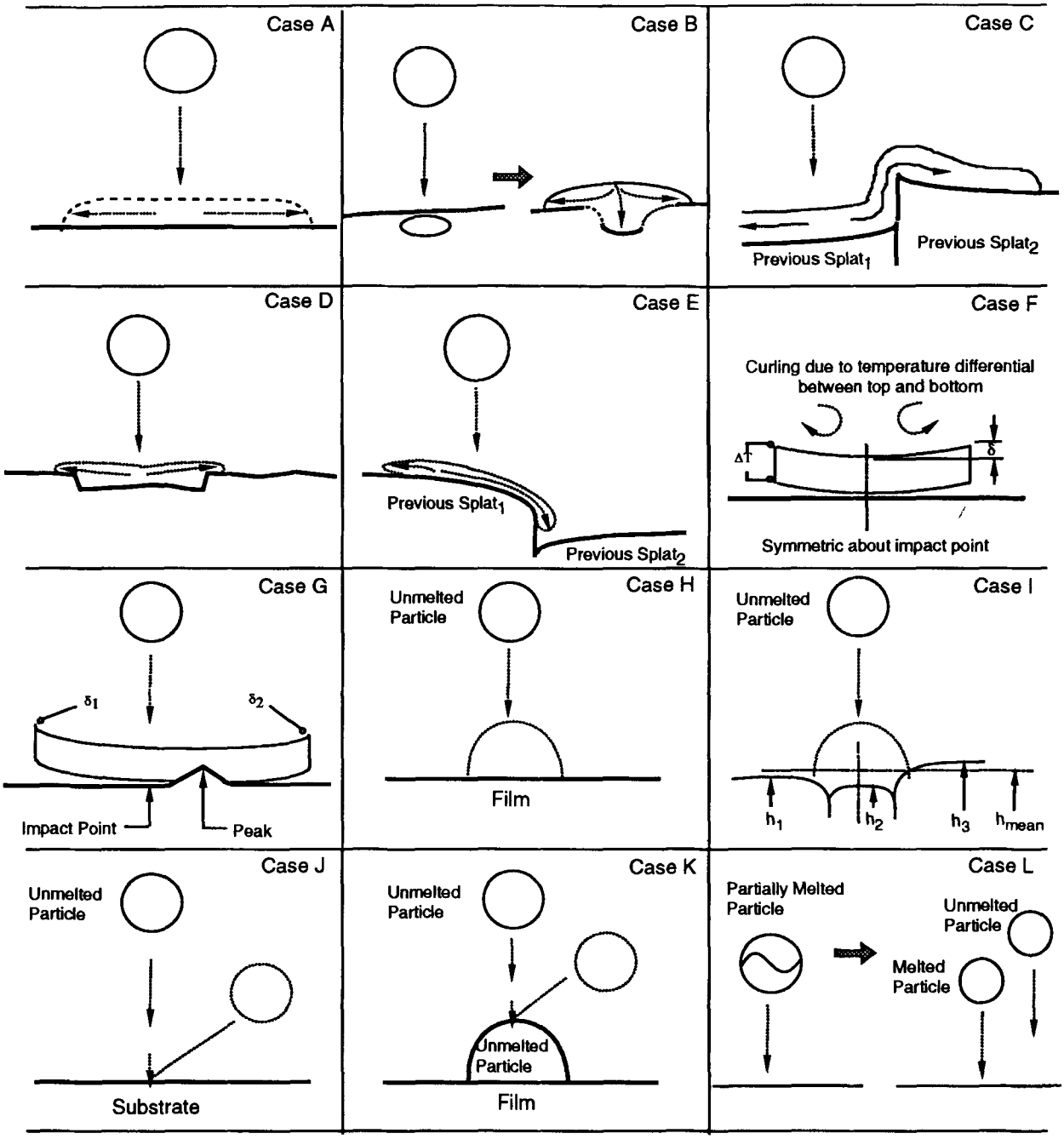

Fig. 5 Rules of deposition model. All views are of the impacting particle and substrate in cross section.

porosity. The porosities from these calculations are approximately half those obtained previously.

Because the program reflects the fact that coating growth is a stochastic process, a number of examples of each set of parameters must be run. Typical values of the standard deviation of the total porosity are in the range of 0.25 to 0.75%. This does not obscure the trends discussed below. It is worthwhile to note that porosity can, at best, be measured to ±1%, so simulation results can be usefully compared with available experimental data. We first define a reference set of parameters for the coating (Table 2), which will be used unless otherwise stated.

The calculations show the strong variation of porosity with coating thickness observed in experiments. Figure 7 presents an example. The porosity close to the interface with the substrate (within 25 μm) is very sensitive to substrate roughness; the typical range of fluctuations is shown in Fig. 7. However, the total porosity is little affected.

The amount of porosity falls as the surface temperature rises (Table 3). The effects of particle diameter and particle velocity are in the same direction as would be expected from the calculations of the splashing of individual particles discussed in Section 2. Thus, the splat diameter increases as the diameter and velocity

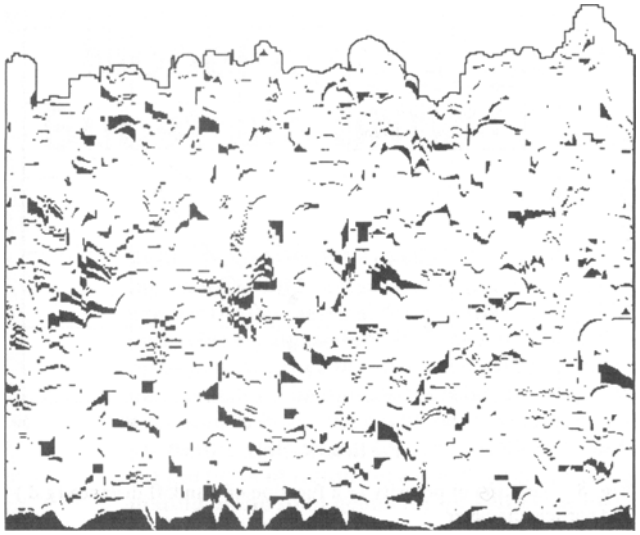

(a)

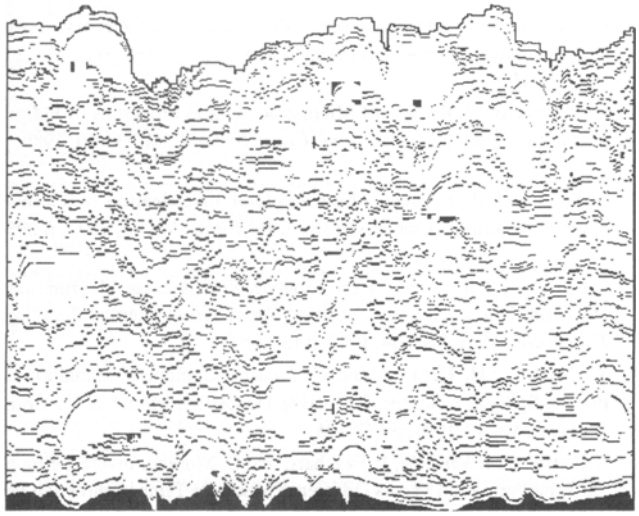

(b)

Fig. 6 Typical simulated coatings for the reference set of parameters (a) For a random distribution of contact parameter f. (b) For a fixed value of $f = 0.2$

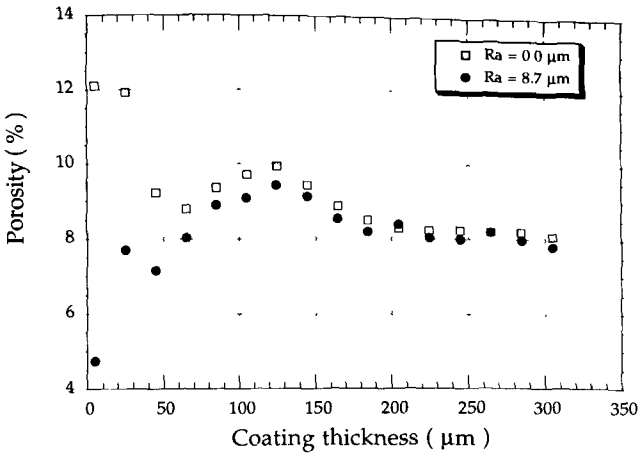

Fig. 7 Distribution of porosity as a function of coating thickness and surface roughness. (a) $R_a = 0.0$ μm. (b) $R_a = 8.7$ μm

Table 2 Reference parameters for simulations

Spraying parameter	Value
Torch power	40 kW
Plasma temperature	2500 K
Surface preheating temperature	773 K
Coating growth rate	1.5 μm/s
Coating thickness	300 μm
Surface temperature	873 K
Particle temperature	3240 ± 284 K
Particle velocity	173 ± 16 m/s
Particle diameter	39 ± 11 μm

Table 3 Effect of surface temperature on porosity

Temperature, K	Porosity, %
300	10.05
500	9.45
700	9.18
900	8.67
1100	7.60
1300	6.73

of the original particle increases. As splat diameter increases, curling also increases (Tables 4 and 5).

However, this complicates the relation between particle diameter and porosity in the real experimental situation. As the experimental correlations show (and as expected on physical grounds), the particle radius and velocity are anticorrelated; large particles move more slowly (Ref 1). Thus, a more complicated picture emerges upon investigating effects such as the variation of porosity as a function of standoff distance (i.e., plasma gun distance) and particle diameter. An example of this is shown in Fig. 8, where correlation data measured by Fauchais et al. (Ref 1) were used. Here the effect of large diameter dominates only at large gun/substrate distances, when the difference in velocities is less. Therefore, when the correlation between process parameters is taken into account, the porosity variations predicted by the model are less pronounced. In the case described in Fig. 8, the calculated variations as a function of standoff distance are buried in the typical scatter of any practical experimental measurement (±1%).

5. Conclusions

A better model of the splashing process has been achieved and the effects on modeling noted. An improved version of the rules for growing the coating has eliminated unphysical correlations observed in the old model (Ref 14). The new model better represents the coating microstructure. The model makes a number of predictions about the relationship between porosity and process parameters.

Table 4 Effect of particle radius on porosity

Radius, μm	Porosity, %
5	3.67
10	6.18
15	6.22
20	7.95
25	10.96

Table 5 Effect of particle velocity on porosity

Velocity, m/s	Porosity, %
50	4.15
75	4.92
100	6.34
150	7.70
200	9.65

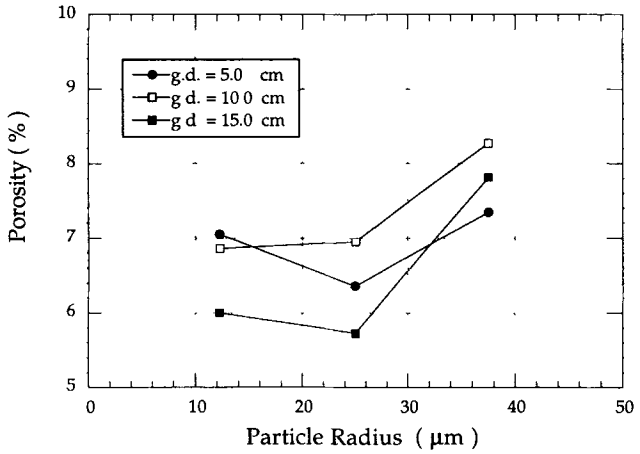

Fig. 8 Variation of porosity as a function of standoff distance (g.d.) and particle diameter

However, little experimental evidence exists to test the detailed predictions beyond the broad assertions that the porosity levels are reasonable and that the behavior as a function of thickness and temperature is sensible. More detailed work is needed to test models of this kind. Work is in progress to obtain such information.

Acknowledgments

The authors wish to acknowledge support from the BRITE/EURAM program of the Commission of European Communities (BRITE, 1991) under Project No. BREU-0418 and also from the Corporate Research Programme of AEA Technology.

References

1. P. Fauchais, A. Grimaud, A. Vardelle, and M. Vardelle, La Projection par Plasma: Une Revue, *Ann. Phys.*, Vol 14, 1989, p 261-310 (in French)
2. G. Trapaga and J. Szekely, Mathematical Modeling of the Isothermal Impingement of Liquid in Spraying Processes, *Metall. Trans. B*, Vol 22B, 1991, p 901-914
3. M. Bertagnolli, M. Marchese, and G. Jacucci, Modeling of Particles Impacting on a Rigid Substrate for Plasma-Sprayed Coatings, *J. Therm. Spray Technol.*, in press
4. A. Vardelle, M. Vardelle, and P. Fauchais, Les Transferts de Quantité de Mouvement et de Chaleur Plasma Particules Solides dans un Plasma d'Arc in Extinction, *Rev. Int. Hautes Temp. Refract.*, Vol 23, 1986, p 69-85 (in French)
5. R. Westhoff, G. Trapaga, and J. Szekely, Plasma-Particle Interactions in Plasma Spraying Systems, *Metall. Trans. B*, Vol 23B, 1992, p 683-693
6. O. Knotek and R. Elsing, Monte Carlo Simulation of the Lamellar Structure of Thermally Sprayed Coatings, *Surf. Coat. Technol.*, Vol 32, 1987, p 261-271
7. H. Fukanuma, An Analysis of the Porosity Producing Mechanism, *Thermal Spray: International Advances in Coatings Technology*, C.C. Berndt, Ed., ASM International, 1992, p 767-772
8. J. Madejski, Solidification of Droplets on a Cold Surface, *J. Heat Mass Transfer*, Vol 19, 1976, p 1009-1013
9. P.Yu. Pekshev and I.G. Murzin, Modelling of Porosity of Plasma Sprayed Materials, *Surf. Coat. Technol.*, Vol 56, 1993, p 199-208
10. P.H. Harmsworth and R. Stevens, Microstructure of Zirconia-Yttria Plasma-Sprayed Thermal Barrier Coatings, *J. Mater. Sci.*, Vol 27, 1992, p 616-624
11. R. McPherson, A Review of Microstructure and Properties of Plasma Sprayed Ceramic Coatings, *Surf. Coat. Technol.*, Vol 39/40, 1989, p 173-181
12. S. Safai and H. Herman, Microstructural Investigation of Plasma-Sprayed Aluminum Coatings, *Thin Solid Films*, Vol 45, 1977, p 295-307
13. S. Kuroda, T. Fukushima, and S. Kitahara, Simultaneous Measurement of Coating Thickness and Deposition Stress during Thermal Spraying, *Thin Solid Films*, Vol 164, 1988, p 157-163
14. S. Cirolini, J.H. Harding, and G. Jacucci, Computer Simulation of Plasma-Sprayed Coatings. I. Coating Deposition Model, *Surf. Coat. Technol.*, Vol 48, 1991, p 137-145
15. S. Fantassi, M. Vardelle, P. Fauchais, and C. Moreau, Investigation of the Splat Formation Versus Different Particulate Temperatures and Velocities prior to Impact, *Thermal Spray: International Advances in Coatings Technology*, C.C. Berndt, Ed., ASM International, 1992, p 755-760
16. G. Trapaga, E.F. Matthys, J.J. Valencia, and J. Szekely, Fluid Flow, Heat Transfer, and Solidification of Molten Metal Droplets Impinging on Substrates: Comparison of Numerical and Experimental Results, *Metall. Trans. B*, Vol 23B, 1992, p 701-718
17. J.M. Houben, "Relation of the Adhesion of Plasma Sprayed Coatings to the Process Parameters Size, Velocity and Heat Content of the Spray Particles," Ph.D. thesis, Technische Universiteit, Eindhoven, The Netherlands, 1988
18. R. McPherson and V. Shafer, Interlamellar Contact within Plasma-Sprayed Coatings, *Thin Solid Films*, Vol 97, 1982, p 201-204
19. L. Pawlowski, M. Vardelle, and P. Fauchais, A Model for the Temperature Distribution in an Alumina Coating during Plasma Spraying, *Thin Solid Films*, Vol 94, 1982, p 307-319
20. L. Bertamini, S. Sturlese, and P. Beber, Atmosphere and Temperature Controlled Spraying (ATCS) of Thermal Barrier Coating on Aluminum Alloys, *Proc. Int. Symp. Automotive Technology and Automization*, Aachen, 1993